

## Hall Coefficient of Potassium Determined by a Helicon Transmission Method\*

D. E. Chimenti and B. W. Maxfield†

Laboratory of Atomic and Solid State Physics, Cornell University, Ithaca, New York 14850

(Received 17 November 1972)

The magnetic field dependence and magnitude of the high-field Hall coefficient of potassium have been determined experimentally by studying the propagation characteristics of high-frequency helicon waves. Between 20 and 100 kG no significant ( $\pm 0.5\%$ ) field dependence is observed in the Hall coefficient for two different crystalline orientations. Absolute measurements yield values which are, depending on the orientation, 4 or 8% larger in absolute value than the free-electron Hall coefficient. Accuracy of the magnitude measurements is estimated at  $\pm 2\%$ . Sample thicknesses are measured *in situ* using a transducerless ultrasonic technique. The temperature dependence of the Hall coefficient has also been measured. To within 0.05% no change in that quantity is observed upon cooling the sample from 4.2 to 2.2 K. The experimental results are discussed in the light of recent theories on the magnetoresistance of potassium which predict a decreasing Hall coefficient with increasing magnetic field.

### I. INTRODUCTION

A long-standing discrepancy exists between transverse magnetoresistance measurements in potassium and semiclassical galvanomagnetic theory. Numerous workers using a variety of experimental techniques have observed a linear term in the high-field magnetoresistance (MR) of both single and polycrystalline potassium.<sup>1</sup> The semiclassical theory of Lifshitz, Azbel, and Kaganov<sup>2</sup> (LAK) cannot yield such a linear term unless a magnetic-field-dependent scattering probability is allowed. Recent attempts to explain the linear MR obtain a field-dependent scattering probability either by magnetic breakdown of open or holelike orbits to closed electron orbits<sup>3,4</sup> or by the less drastic process of magnetic-field-induced umklapp scattering.<sup>5</sup>

A consequence of theories which rely on magnetic breakdown of open or holelike orbits to explain a linear MR is that they also give a field-dependent Hall coefficient  $R_H$ . Such behavior has been observed in potassium by Penz and Bowers<sup>6</sup> using a low-frequency helicon-standing-wave technique; they find that above about 20 or 40 kG,  $R_H$  decreases with increasing magnetic field  $B$ .<sup>7</sup> At 110 kG the decrease amounts to about 7%. Their measurements of the absolute value of  $R_H$  show a 6–12% enhancement over the free-electron value  $R_{H,FE}$ , deduced from an x-ray determination of the lattice constant.<sup>8</sup> When the appropriate finite specimen correction factor<sup>9</sup> is applied to these and previous helicon measurements of  $R_H$ ,<sup>10</sup> agreement with  $R_{H,FE}$  is obtained within the experimental uncertainties of a few percent. The semiclassical LAK<sup>2</sup> theory predicts that the high-field Hall coefficient of a closed-orbit uncompensated metal should be independent of magnetic field and inversely proportional to the effective carrier density. Goodman,<sup>11</sup> using the appropriate solution of the

boundary-value problem calculated by Legendy,<sup>12</sup> deduces a value of  $R_H$  at 25 and 35 kG from helicon measurements on long polycrystalline cylinders which agrees with  $R_{H,FE}$  to within  $\frac{1}{2}\%$ . Direct-current experiments on  $R_H$  in potassium are summarized by Alderson and Farrell,<sup>13</sup> whose own results on the temperature dependence of  $R_H$  extend from 6 to 300 K. The accuracy of their absolute measurement is 4%, and agreement with  $R_{H,FE}$  is obtained to within 2% at 6 K. All of the above results quoted for  $R_H$  are in the high-field limit.

It is the purpose of the current study to measure the absolute high-field Hall coefficient and its field dependence between 20 and 100 kG in single-crystal potassium and to avoid the shortcomings of both the direct-current experiments and the standing-wave helicon method. We have studied high-frequency helicon-wave propagation through plates of thickness  $d > 50\lambda$ , where  $\lambda$  is the helicon wavelength. From the field-dependent helicon transmission characteristics, we have been able to deduce  $R_H$  with 2% absolute accuracy and field and temperature changes in  $R_H$  to better than  $\frac{1}{2}\%$  accuracy at  $T = 4.2$  K.

In Sec. II we summarize the basic theory necessary for the interpretation of our measurements. Section III describes the various experimental techniques that were employed, and Sec. IV discusses the pertinent aspects of data reduction. The results and discussion are presented in Sec. V.

### II. THEORY AND METHOD

The helicon is a transverse circularly polarized electromagnetic wave which can propagate in an uncompensated closed-orbit metal under the following conditions of low damping: (i)  $\omega_c\tau \gg 1$ , where  $\omega_c = eB/m^*$  is the cyclotron frequency,  $e$  is the electronic charge,  $B$  is the flux density,  $m^*$

is the carrier effective mass, and  $\tau$  is the electronic relaxation time; (ii)  $\vec{q} \cdot \vec{v}_F < \omega_c$ , where  $\vec{q}$  is the helicon wave vector and  $\vec{v}_F$  is the Fermi velocity. The first condition places a lower limit on the magnetic field and is analogous to the requirement that the helicon wave vector be largely real. At constant field the second condition sets an upper limit on the helicon frequency. For  $\vec{q} \cdot \vec{v}_F = \omega_c$  the charge carriers undergo Doppler-shifted cyclotron resonance, and when  $|\vec{q}| |\vec{v}_F| > \omega_c$  the helicon will be strongly damped as a result of this resonant absorption.

To calculate the dispersion relation, we begin with the nonlocal scalar wave equation derived by Baraff,<sup>14</sup>

$$\left( \frac{d^2}{dz^2} + \frac{\omega^2}{c^2} \right) E(z) = -i\omega\mu_0 \int_{-\infty}^{\infty} \sigma(|z-z'|) E(z') dz', \quad (1)$$

where  $\omega$  is the angular frequency of the helicon,  $\sigma(|z-z'|)$  is the nonlocal conductivity,  $\mu_0$  is the permittivity of free space,  $c$  is the speed of light, and  $E(z)$  is the electric field anywhere in the infinite medium. Propagation along the static magnetic field, which is parallel to the  $z$  direction, has been assumed. Implicit in Eq. (1) is the assumption that the metal may be adequately represented as a free-electron gas. Following Baraff,<sup>14</sup> one substitutes the infinite-medium conductivity of Reuter and Sondheimer,<sup>15</sup> which is derived for free-electron charge carriers in the standard relaxation-time approximation. After evaluation of the integrals, Eq. (1) reduces to

$$q_{\pm}^2 - \frac{\omega^2}{c^2} - \frac{3}{4} \frac{\mu_0 \omega n e^2}{q_{\pm} \hbar k_F} \times \left[ \frac{2}{b_{\pm}} + \left( 1 - \frac{1}{b_{\pm}^2} \right) \ln \left( \frac{1+b_{\pm}}{1-b_{\pm}} \right) \right] = 0, \quad (2)$$

where  $n$  is the electron density and  $\hbar k_F$  is the Fermi momentum. The  $(\pm)$  refers to left- or right-circular polarization, only one of which will propagate depending on the sign of the charge carrier and the direction of the magnetic field. The term  $b_{\pm}$  is given by

$$b_{\pm} = -qv_F / (\mp \omega_c + i/\tau), \quad (3)$$

where  $\omega$  has been neglected compared to  $\omega_c$ . It is understood that the logarithm vanishes when  $|b_{\pm}| = 0$ . Similar derivations are given by Platzman and Buchsbaum<sup>16</sup> and Miller and Haering.<sup>17</sup>

As it stands, Eq. (2) is not in a convenient form for computation. Exploiting the fact that  $\omega_c \tau \gg 1$  (generally no less than 40) and  $|b_{\pm}| < \frac{1}{2}$ , one obtains a simple expression which is still accurate to order  $(\omega_c \tau)^{-2}$ . The logarithm is expanded, and the following approximation is substituted in Eq. (3):

$$\text{Re}(q_{\pm})^2 / \text{Im}(q_{\pm})^2 \approx \omega_c \tau. \quad (4)$$

Keeping only the dispersive real part and suppressing the polarization notation, Eq. (2) may be rewritten

$$q^2 = (\omega \mu_0 / R_H B) \left( 1 + \frac{1}{5} w^2 + \frac{3}{35} w^4 + \dots \right), \quad (5)$$

where

$$w = qv_F / \omega_c \quad (6)$$

and  $q$  is understood to be entirely real. Note that within the abovementioned limitations, this result is valid for all  $ql$ <sup>18</sup>;  $l$  is the mean free path.

In our transmission experiment we employ the rectangular-plate geometry, generating the helicon by inducing currents in the skin depth on one side of the slab and detecting the emergent helicon magnetic field at the other. Since high frequencies are used (2–10 MHz), the finite-slab effects calculated by Legendy<sup>12</sup> can be shown to be negligible compared to experimental uncertainty, and therefore the infinite-medium dispersion relation, Eq. (2), is a valid approximation.

An important feature of this experiment is our determination of the specimen thickness which is performed simultaneously with the helicon experiment and in the same apparatus. An acoustic shear wave propagating normal to the surface is created by an electromagnetic generation process.<sup>19</sup> From the time of flight of the acoustic pulse and the known elastic constants of potassium,<sup>20</sup> the thickness of the specimen can be inferred. It is worth noting that a sound wave generated in this manner measures the actual distance between the two surface-current sheets in which the generation and detection of the helicon occur.

### III. EXPERIMENTAL TECHNIQUE

Our experiment utilizes the conventional helicon transmission geometry depicted in Fig. 1. Small spiral coils, which serve to generate both the helicon and acoustic waves, are embedded in epoxy and held parallel in copper irises. The coils are placed on either side of the flat-plate specimens, which are typically  $12 \times 12 \times 2.5$  mm. As shown in Fig. 2, the copper rings slide on two stainless-steel tracks to permit damage-free mounting and demounting of the specimens. Wound from No. 38 copper wire, the coils are Formvar insulated, and connections to them are made via two well-shielded balanced transmission lines. These lines consist of Teflon-insulated twisted pairs of No. 30 copper wire about 1 m long and potted with epoxy in stainless-steel tubes. Low-loss ferrite-core isolation transformers placed in brass housings provide coupling to single-ended sources and amplifiers. With this arrangement the zero-field ratio of direct-leakage voltage to drive voltage can be made less than  $-110$  dB. The magnetic field is measured with a 2500-turn magnetoresistance

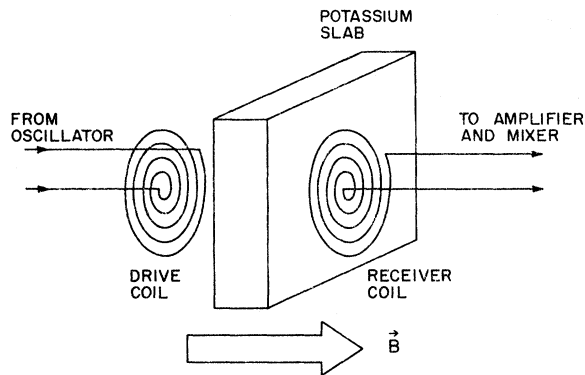


FIG. 1. Coil-sample arrangement. The coil windings are approximately 0.25 mm from the sample surface.

probe wound bifilarly from No. 46 copper wire and positioned within 1.3 cm of the specimen. The probe is NMR calibrated from 20 to 100 kG. Reproducibility to 0.1% has been verified during the course of several runs.

All specimens for these measurements have been prepared from high-purity potassium.<sup>21</sup> Typical values for the residual resistance ratio are about 3000, as measured by the eddy-current-decay method.<sup>22</sup> The large single-crystal boules from which the specimens were ultimately cut are grown by a standard Bridgman technique described in detail by Taub.<sup>23</sup> Potassium, in a sealed glass ampoule from the supplier, is melted under vacuum ( $\sim 10^{-4}$  Torr) into a clean tapered glass crucible which has been lightly coated with dry outgassed paraffin oil. Maintained at slightly above the melting point for 8–10 h, the metal is allowed to outgas at  $10^{-5}$  Torr. After a cooling cycle of about 3 h, the boule, which slides easily from the crucible, is etched and examined for grain boundaries. Orientation to within  $1^\circ$  is accomplished by x-ray Laue-transmission methods using the radiographs for a bodycentered-cubic lattice published by Majima and Togino.<sup>24</sup> With the oriented crystal mounted on a goniometer, slices are taken with a string saw using a mixture of water and alcohol for the etch. At each stage, care is exercised to prevent unnecessary straining of the specimens.

The final preparation of the specimen surfaces is accomplished in one of two ways. In the first method, the rectangular plate is successively mounted in two stainless-steel lapping rings, 3- and 2.5-mm deep. Using only the weight of the rings, the crystals are gently hand lapped on bond paper soaked with paraffin oil and secondary butyl alcohol. This procedure produces high-quality surfaces only occasionally; also, there is a possibility of introducing strains. A more sophisticated method of preparing smooth surfaces involves the use of a crystal-facing instrument.<sup>25</sup> This de-

vice consists of a vertically mounted stainless-steel lapping wheel 25 cm in diameter, over which high-grade wool cloth is stretched. The polishing solution of isopropanol, paraffin oil, and xylene in a proportion of 9:6:1 fills a container through which the wheel passes. A roller regulates the amount of solution left on the cloth. Paraffin wax secures the specimen in a shallow stainless-steel cup, and the rotating sample assembly is suspended against the wheel by thin stainless-steel bands, which allow a small, but reproducible, lapping pressure to be sustained. Both wheel and sample mount are motor driven asynchronously, averaging any bias in the wheel's rotation. After lapping, the surface is immediately washed with xylene and protected with dry petroleum jelly. The procedure is repeated for the opposite surface, taking care not to degrade the one already prepared. With this method we achieve surface flatness conservatively estimated, from ultrasonic pulse-echo measurements, at 0.01 mm. The sample is then dismantled from its holder and cleaned thoroughly in xylene. When the last traces of jelly are removed, the specimen is slowly cooled<sup>26</sup> to  $0^\circ\text{C}$ , then dried with a tissue and cooled to 77 K where it is stored until needed.

A block diagram of the instrumentation employed in this experiment is shown in Fig. 3. An amplitude-modulated radio-frequency (rf) signal of stable frequency is fed to a power amplifier and

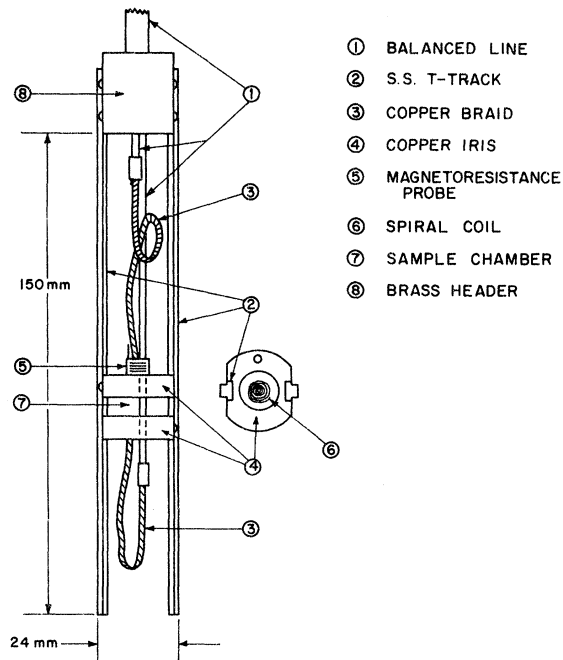


FIG. 2. Schematic of the apparatus. The balanced transmission lines are brought to the spiral coil through flexible copper braid to allow adjustment of the irises.

the reference channel of an rf mixer. The amplifier output drives the transmitter coil producing a helicon wave which propagates to the far surface where it is detected by the receiver coil. After 60 dB of amplification and some filtering, the pick-up voltage goes to the signal channel of the mixer where it is phase-sensitively detected. The 1-kHz amplitude modulation of the rf is then removed by a final phase-sensitive detection. If desired, the resulting signal can be actively differentiated to remove a linear-field-dependent background voltage that is sometimes present (possibly caused by the magnetoresistance of the potassium). Since the magnetic field is varied linearly in time, the differentiation gives a field derivative. The signals from the MR field probe and either the phase-sensitive detector or the differentiator are fed to an X-Y recorder. This method is described in more detail by Hansen, Grimes, and Libschaber.<sup>27</sup>

Two superconductive solenoids are used in this experiment. The first produces a maximum field of 55 kG with a homogeneity of about 0.5% in a 2-cm diameter spherical volume (dsv). A constant-current supply controlled by a linear voltage ramp powers the magnet. The second is a 100-kG solenoid manufactured by General Electric Corp. and produces a field homogeneous to better than 0.1% in a 2-cm dsv. This magnet is driven by a superconductive-flux pump.

As mentioned previously, the sample thickness is determined in the same apparatus as that used for the helicon measurements. The instrumentation, however, differs. Briefly, a 0.5- $\mu$ sec duration 10-MHz pulse is delivered to the drive coil, and simultaneously, a gated integrating

amplifier receives a trigger signal. The receiver-coil voltage passes through a multistage i.f. amplifier, then a detector, and finally to the gated amplifier. This permits the echo-decay pattern to be recorded. Similar ultrasonic methods are discussed more extensively elsewhere.<sup>28</sup>

#### IV. DATA ANALYSIS

Equation (5) gives the relationship between  $R_H$  and the helicon wave vector  $q$ . From the expression for the transmitted helicon magnetic field,<sup>29</sup>

$$b_z = [(\xi i/z) \sin qd + \cos qd]^{-1} b_i, \quad (7)$$

where  $d$  is the sample thickness,  $b_i$  is the excitation field, and  $\xi (\gg 1)$  is the refractive index of the metal, it follows that  $b_z$  assumes an extremum whenever

$$qd = n\pi. \quad (8)$$

From Eqs. (5) and (8),

$$R_H = (\mu_0 \omega d^2 / n^2 \pi^2 B_n) f(w), \quad (9)$$

where  $w$  is defined by Eq. (6),  $B_n$  is the field of the  $n$ th extremum, and  $f(w)$  is the so-called nonlocal correction factor. Once the fringe index  $n$  has been established, the absolute value and field dependence of  $R_H$  may be calculated from Eq. (9). Figure 4 shows that  $b_z$  is a smooth function of  $B$ , having the expected shape and symmetry. The position of the extrema may be determined with an accuracy greater than 0.1%.

The assignment of  $n$  is accomplished by performing a least-squares linear fit on  $(n', B_n^{-1/2})$  data pairs, where  $n'$  is a trial value for the fringe index. By shifting the values of  $n'$  in the data pairs until

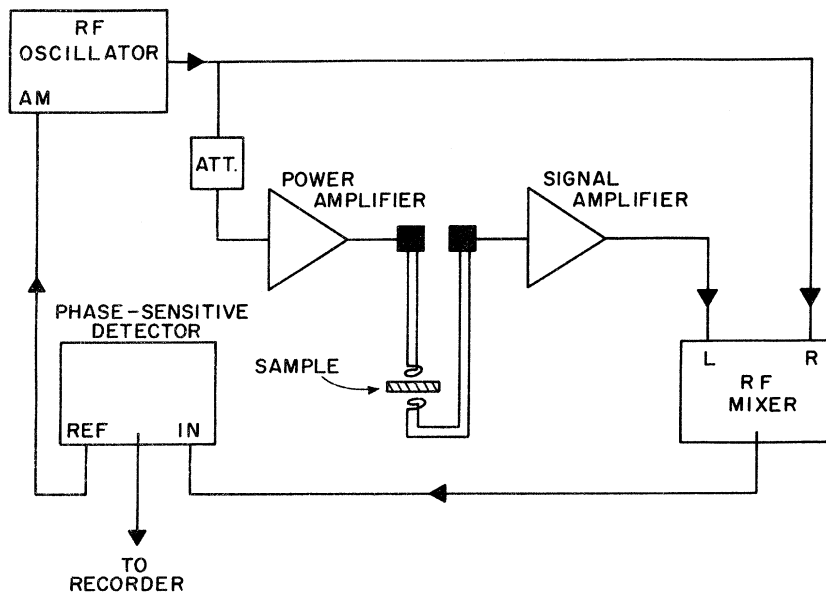


FIG. 3. Experimental instrumentation employed in high-frequency helicon studies.

$n \rightarrow 0$  as  $B_n^{1/2} \rightarrow \infty$ , a determination of  $n$  can be made with an error of  $\pm \frac{1}{2}$ . As a check, fringe indices are computed separately for low-, intermediate-, and high-field regions. In each case nonlocal effects are included. These independent predictions, which tend to eliminate any bias implicit in the analysis, can then be compared for consistency. To obtain the best fit possible, the range of  $B_n$  is restricted to regions where  $b_t$  displays good symmetry, such as shown in Fig. 4. The best predictions of  $n$  for a single spectrum never differ by more than  $\pm 1$ .

To obtain the magnetic field from the resistance of the field probe, a functional relationship of the form

$$B = A(\Delta R)^x, \quad (10)$$

where  $\Delta R$  is the change in probe resistance in a field  $B$ , is assumed for the ten or so calibration points between 25 and 100 kG. The parameters  $A$  and  $x$  are determined by a least-squares fit. Higher accuracy is achieved by adding a polynomial correction term to the right-hand side of Eq. (10) and minimizing the small deviation between it and the calibration values. Absolute errors in the magnitude of  $B$  are estimated at 0.2%, while relative errors are considerably smaller.

For all measurements of sample thickness, the shear velocity corresponding to particle motion along a fourfold symmetry axis is chosen. It has been verified by solution of the equations of motion for acoustic propagation in a general direction that this mode is least sensitive to small misorientation which might occur in cutting the sample from the boule or in preparation of the surfaces. The accuracy of the thickness measurement is estimated to be 0.5%, assuming no error in the elastic con-

stants. Sample dimensions have been checked independently with a micrometer at 77 K, allowing 25  $\mu$  for the thickness of the oxide layer. The average difference between the mechanical and ultrasound results is approximately 0.5%.

## V. RESULTS AND DISCUSSION

Figure 5 shows the field dependence of  $R_H$  in single-crystal potassium. In Fig. 5(a) results for samples 13 and 16, normalized to the value of  $R_H$  at 50 kG, are displayed. They cover a range of magnetic field from 25 to 95 kG, with the static magnetic field directed along a [110] axis. Note the smooth overlap between 40 and 50 kG and the relative lack of any field dependence. We consider structure at the  $\frac{1}{2}\%$  level in this and following curves not to be significant. Further [110] results are given in Fig. 5(b). Here, we observe about a 1% change in  $R_H$  between 20 and 90 kG in two different runs on sample 15 at 4.2 K.

Results of measurements on single crystals oriented with the magnetic field directed along a [100] axis also appear in Fig. 5. Figure 5(c) shows the results of a high-field run at 12 MHz and a low-field run at 3.3 MHz performed on samples 18 and 19, respectively. No field dependence (within experimental error) is observed from 24 to 100 kG. Results of a third [100] sample are presented in Fig. 5(d); no significant field dependence in  $R_H$  appears in two runs, one at 2 MHz, the other at 12.5 MHz. In fact, only in the results of sample 15 do any data points lie farther from the abscissa than the experimental error of  $\pm \frac{1}{2}\%$ .

The observation of a field-independent Hall coefficient presented above may be contrasted with the data of Penz and Bowers.<sup>8</sup> In a single-crystal specimen, no field dependence was observed from

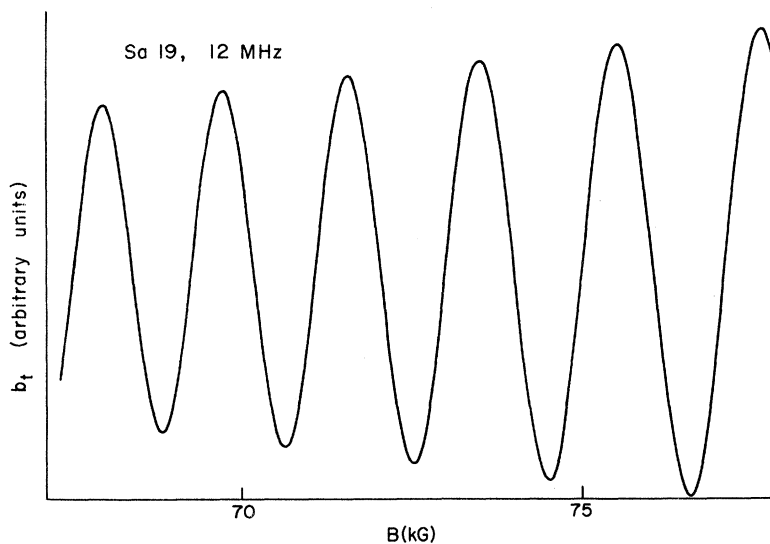


FIG. 4. Transmitted helicon signal vs magnetic field. The magnitude increases with field because of the reduction in collisional damping.

10 to 20 kG, but between 20 and 55 kG a 3% decrease was seen. Polycrystalline samples exhibit a change of about 1% in  $R_H$  from 10 to 60 kG, then a steep descent of 6% from 60 to 110 kG.

More recently, induced-torque measurements in potassium by Schaefer and Marcus<sup>30</sup> indicate the presence of a nonsaturating torque with increasing magnetic field. In an uncompensated metal the induced torque in the high-field limit on a sphere has the same field dependence as the transverse MR.<sup>31</sup> Overhauser<sup>32</sup> has presented an explanation of this anomalous behavior in which open orbits are responsible for the nonsaturating torque. There is evidence, however, that in spite of the induced-torque anomalies, potassium has a simply connected Fermi surface.<sup>33</sup> Nonlocal-helicon-damping measurements carried out by Houck and Bowers<sup>34</sup> on polycrystalline potassium indicate a close agreement with the prediction of free-electron theory. In principle, helicon damping should be very sensitive to the connectivity of the Fermi surface.<sup>35</sup> Earlier, Reitz and Overhauser<sup>3</sup> discussing the MR of potassium referred to specific model calculations of Falicov and Sievert<sup>36</sup> which apply to magnetic breakdown of closed hole to closed electron orbits. This case was chosen by Reitz and Overhauser to explain the observations in potassium because it can yield a linear MR over a fairly wide range of magnetic field. O'Keefe and Goddard<sup>4</sup> proposed a similar scheme for lithium. Our results, showing no significant field dependence in the high-field Hall coefficient from 20 to 100 kG, have relevance for the proposals which seek to explain the linear transverse MR of potassium by the mechanism of magnetic breakdown of open or holelike orbits. The absence of any substantial field dependence in  $R_H$ , which mea-

sures the difference of electron and hole concentrations, could show either that the postulated breakdown field of about 50 kG<sup>3,37</sup> is too low, or that the mechanism responsible for the linear MR in potassium is not related to magnetic breakdown. In the first instance a problem arises if a larger breakdown field (consistent with our results) is used in the model calculations. In that case the onset of the linear term in the MR will be shifted to higher fields. Experimentally, however, the linear term persists from approximately 10 kG to at least 100 kG.<sup>1</sup> Thus, the proposals which rely on magnetic breakdown seem to be inconsistent with the observation of a linear MR at low fields and a nearly field-independent Hall coefficient up to 100 kG.

Turning to measurements of the absolute value of  $R_H$ , our results are given in Table I. Within each orientation the magnitudes are in fairly close agreement. In the [100] direction we find that  $R_H$  is about 4% greater than  $R_{H,FE}$ . For the [110] direction the enhancement is 7 or 8%. One possible source of systematic error in the magnitude of  $R_H$  is the sound-velocity measurement performed by Marquardt and Trivisonno.<sup>20</sup> These workers claim for their results a precision of 1 or 2%. Since the sample thickness enters the expression for  $R_H$  quadratically [Eq. (9)], any error in the fast shear sound velocity will be reflected doubly in our values of  $R_H$ . However, it should be noted that the ratio of  $R_H$  in the [110] samples to  $R_H$  in the [100] samples is independent of the sound velocity, since the [100] shear wave and the [110] fast shear wave both correspond to particle motion along a [100] axis. Thus, the apparent anisotropy can be confirmed to a higher accuracy than the absolute magnitude of  $R_H$  in either

TABLE I. Measured absolute values of the Hall coefficient of potassium. All values were determined at a magnetic field of 50 kG.

Sample	$[hkl]$ <sup>a</sup>	$\nu$ (MHz) <sup>b</sup>	$d$ (mm) <sup>c</sup>	$R_H$ ( $10^{-10}$ m <sup>3</sup> /C)	$\frac{R_H - R_{H,FE}}{R_{H,FE}} \times 100$
13	[110]	2.0	2.48	4.73	6 $\frac{1}{3}$
15	[110]	7.0	2.38	4.79	7 $\frac{1}{2}$
15	[110]	10.0	2.38	4.82	8 $\frac{1}{3}$
16	[110]	6.8	2.40	4.80	8
17	[100]	6.0	2.62	4.60	3 $\frac{1}{2}$
18	[100]	3.3	1.65	4.74	6 $\frac{1}{2}$
18	[100]	7.3	1.65	4.68	5
19	[100]	10.0	2.825	4.65	4 $\frac{1}{2}$
19	[100]	12.0	2.825	4.61	3 $\frac{1}{2}$
20	[100]	2.0	3.17	4.60	3 $\frac{1}{2}$
20	[100]	7.8	3.17	4.61	3 $\frac{1}{2}$
20	[100]	12.5	3.17	4.65	4 $\frac{1}{2}$

<sup>a</sup> $[hkl]$  represents the crystallographic indices of the magnetic field and the sample normal.

<sup>b</sup> $\nu$  is the approximate helicon frequency.

<sup>c</sup> $d$  is the sample thickness.

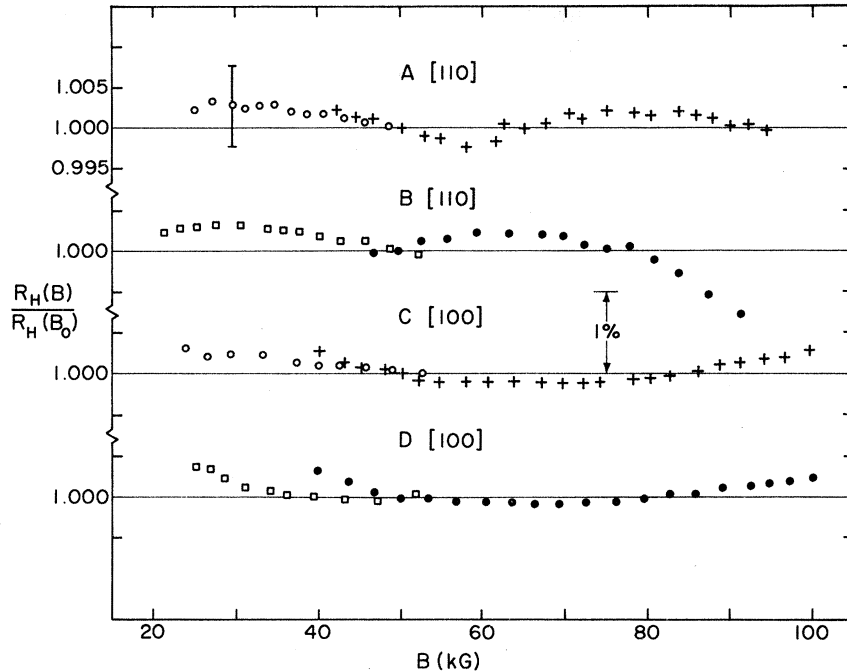


FIG. 5. Hall coefficient of potassium vs magnetic field.  $B_0=50$  kG; (a):  $\circ$  sample 13, 2 MHz;  $+$  sample 16, 6.8 MHz; (b):  $\square$  sample 15, 7 MHz;  $\bullet$  sample 15, 10 MHz; (c):  $\circ$  sample 18, 3.3 MHz;  $+$  sample 19, 12 MHz; (d):  $\square$  sample 20, 2 MHz;  $\bullet$  sample 20, 12.5 MHz. The experimental uncertainty is indicated on line (a) by a typical error bar. See Table I for absolute values.  $T=4.2$  K.

crystal orientation.

Striking agreement with semiclassical theory is observed in the temperature dependence of  $R_H$ . By performing the experiment on the same sample and at the same frequency, resolution of better than 0.1% can be achieved since the only limiting factors are the noise on the transmitted helicon signal (see Fig. 4) and the reproducibility of the field probe. The sample was cooled from 4.2 to 2.2 K. Although a significant decrease in thermal scattering occurs with this temperature variation,<sup>38</sup> no change in either the absolute value or field dependence of  $R_H$  between 30 and 52 kG could be observed to an accuracy of 0.05%. The galvanomagnetic theory of LAK<sup>2</sup> predicts that no field-independent scattering process can influence the Hall coefficient of a closed-orbit metal in the high-field limit.

The interpretation of the absolute measurements presented in Table I is somewhat clouded by the relatively large uncertainty, perhaps 3 or 4%, when one includes the probable error in the sound-velocity (thickness) measurements. Nonetheless, there seems to be a definite trend in the data indicating an enhancement over  $R_{H,FE}$  of a few percent, and therefore a departure from free-electron theory. In this connection a sample of single-crystal indium has been run to test the reliability of our method. An average decrease in  $R_H$  of about  $1\frac{1}{2}\%$  with increasing field is observed between 30 and 50 kG at several helicon frequencies. This field dependence is in qualitative agreement with the results of Garland and Bowers,<sup>39</sup> using a dc tech-

nique. Micrometer calipers were used to obtain the dimension of the randomly oriented single-crystal sample, and the measured absolute value of  $R_H$  is found to be  $(1.66 \pm 0.05) \times 10^{-10} \text{ m}^3/\text{C}$ . The high-field value for indium is  $1.60 \times 10^{-10} \text{ m}^3/\text{C}$ . It should be noted that the presence of open or hole-like orbits in potassium would lead to a Hall coefficient that is larger than  $R_{H,FE}$  by the fraction of carriers in open orbits or by twice the fraction of carriers in holelike orbits. Estimates of the possible enhancement range from 10 to 15%.<sup>32,37</sup>

In conclusion, the current study has sought to provide an accurate determination of the field dependence and absolute value of  $R_H$  in potassium, while avoiding ambiguities of the low-frequency helicon method and probe effects inherent in the dc method. We have used the propagation characteristics of high-frequency helicon waves to infer the field dependence of  $R_H$  and, together with a dimension measurement employing electromagnetically generated ultrasound, the absolute value. Our results with the static magnetic field directed along a [100] and a [110] axis show no field dependence in  $R_H$  from 20 to 100 kG within the experimental error of  $\pm 0.5\%$ . In the absolute-value measurements we find  $R_H$  to be larger than the free-electron value for potassium by about 3 or 4% in the [100] samples and by about 8% in the [110] samples. While we feel confident that the absence of a field dependence in the Hall coefficient rules out magnetic breakdown as an explanation of the linear magnetoresistance in potassium, the possible existence of open orbits cannot be rejected.

## ACKNOWLEDGMENT

The authors wish to express their gratitude to

John Peech for the generous loan of his crystal-faceting instrument and for his valuable assistance in developing sample preparation techniques.

\*Work supported mainly by the U. S. Atomic Energy Commission under Contract No. AT(11-1)-3150, Technical Report No. C00-3150-9. Additional support was received from the Advanced Research Projects Agency and the National Science Foundation through use of the technical facilities of the Materials Science Center, Cornell University, MSC Report No. 1910.

†Alfred P. Sloan Research Fellow.

<sup>1</sup>For a review of previous work, see H. Taub, R. L. Schmidt, B. W. Maxfield, and R. Bowers, *Phys. Rev. B* **4**, 1134 (1971).

<sup>2</sup>I. M. Lifshitz, M. Ya. Azbel, and M. I. Kaganov, *Zh. Eksp. Teor. Fiz.* **30**, 220 (1955) [*Sov. Phys.-JETP* **3**, 143 (1956)]; *Zh. Eksp. Teor. Fiz.* **31**, 63 (1956) [*Sov. Phys.-JETP* **4**, 41 (1957)].

<sup>3</sup>J. R. Reitz and A. W. Overhauser, *Phys. Rev.* **171**, 749 (1968).

<sup>4</sup>P. M. O'Keefe and W. A. Goddard, III, *Phys. Rev. Lett.* **23**, 300 (1969).

<sup>5</sup>R. A. Young, *Phys. Rev.* **175**, 813 (1968); L. M. Falicov and H. Smith, *Phys. Rev. Lett.* **29**, 124 (1972).

<sup>6</sup>P. A. Penz and R. Bowers, *Phys. Rev.* **172**, 991 (1968).

<sup>7</sup>Of course, electrons are the dominant charge carriers in potassium, but  $R_H$  has been assumed to be positive for convenience.

<sup>8</sup>C. S. Barrett, *Acta Crystallogr.* **9**, 671 (1956).

<sup>9</sup>T. Amundsen, *Proc. R. Soc. Lond.* **88**, 757 (1966).

<sup>10</sup>R. G. Chambers and B. K. Jones, *Proc. R. Soc. A* **270**, 417 (1962).

<sup>11</sup>J. M. Goodman, *Phys. Rev.* **171**, 641 (1968).

<sup>12</sup>C. R. Lengendy, *Phys. Rev.* **135**, A1713 (1964).

<sup>13</sup>J. E. A. Alderson and T. Farrell, *Phys. Rev.* **185**, 876 (1969).

<sup>14</sup>G. A. Baraff, *Phys. Rev.* **178**, 1155 (1969).

<sup>15</sup>G. E. H. Reuter and E. H. Sondheimer, *Proc. R. Soc. A* **195**, 336 (1948).

<sup>16</sup>P. M. Platzman and S. J. Buchsbaum, *Phys. Rev.* **132**, 2 (1963).

<sup>17</sup>P. B. Miller and R. R. Haering, *Phys. Rev.* **128**, 126

(1962).

<sup>18</sup>M. T. Taylor, *Phys. Rev.* **137**, A1145 (1965).

<sup>19</sup>J. R. Houck, H. V. Bohm, B. W. Maxfield, and J. Wilkins, *Phys. Rev. Lett.* **19**, 224 (1967).

<sup>20</sup>W. R. Marquardt and J. Trivisonno, *J. Phys. Chem. Solids* **26**, 273 (1965).

<sup>21</sup>Supplied by MSA Research Corp., Evans City, Pa. 16033.

<sup>22</sup>C. P. Bean, R. W. DeBlois, and L. B. Nesbitt, *J. Appl. Phys.* **30**, 1976 (1959).

<sup>23</sup>H. J. Taub, Ph.D. thesis (Cornell University, 1971) (unpublished).

<sup>24</sup>M. Majima and S. Togino, *Sci. Pap. Inst. Phys. Chem. Res. Tokyo* **7**, 259 (1927).

<sup>25</sup>Available from South Bay Technology, Inc., 4900 Santa Anita Avenue, El Monte, Calif. 91731.

<sup>26</sup>J. W. Ekin, Ph.D. thesis, (Cornell University, 1971) (unpublished).

<sup>27</sup>J. W. Hansen, C. C. Grimes, and A. Libschaber, *Rev. Sci. Instrum.* **38**, 895 (1967).

<sup>28</sup>R. F. S. Hearmon, *Rev. Mod. Phys.* **18**, 409 (1946).

<sup>29</sup>P. A. Penz, *J. Appl. Phys.* **38**, 4047 (1967).

<sup>30</sup>J. A. Schaefer and J. A. Marcus, *Phys. Rev. Lett.* **27**, 935 (1971).

<sup>31</sup>P. B. Visscher and L. M. Falicov, *Phys. Rev. B* **2**, 1518 (1970).

<sup>32</sup>A. W. Overhauser, *Phys. Rev. Lett.* **27**, 938 (1971).

<sup>33</sup>D. Shoenberg and P. J. Stiles, *Proc. R. Soc. A* **281**, 62 (1964).

<sup>34</sup>J. R. Houck and R. Bowers, *Phys. Rev.* **166**, 397 (1968).

<sup>35</sup>E. A. Kaner and V. G. Skobov, *Adv. Phys.* **17**, 605 (1968).

<sup>36</sup>L. M. Falicov and P. R. Sievert, *Phys. Rev.* **138**, A88 (1965).

<sup>37</sup>A. W. Overhauser, *Bull. Am. Phys. Soc.* **17**, 40 (1972).

<sup>38</sup>J. W. Ekin and B. W. Maxfield, *Phys. Rev. B* **4**, 4215 (1971).

<sup>39</sup>J. C. Garland and R. Bowers, *Phys. Rev.* **188**, 1121 (1969).

## Phase-Shift Analysis of Impurity Scattering in Copper

P. T. Coleridge

*Division of Physics, National Research Council of Canada, Ottawa, Ontario K1A 0R6, Canada*

(Received 27 October 1972)

An identity is proved that allows impurity scattering to be calculated in terms of partial waves by using conventional band-structure programs. It is particularly simple when used in conjunction with a phase-shift parametrization of the Fermi surface and it then conveniently gives the average scattering as sampled by the de Haas-van Alphen effect. The technique is illustrated by applying it to impurity scattering in copper.

There has recently been some interest in parametrizing Fermi surfaces with band-structure calculations by adjusting the phase shifts, which characterize the scattering of the muffin-tin potentials, to obtain agreement with experimentally

measured areas. It has been demonstrated in some detail<sup>1-4</sup> that not only can an accurate fit to the Fermi surface be obtained with the first few phase shifts ( $l=0, 1, 2$  in copper) but also the accuracy is remarkably independent of the choice of the energy